A Proactive Task Set Influences How Response Inhibition Is Implemented in the Basal Ganglia

Inge Leunissen,[1]* James P. Coxon,[2,3] and Stephan P. Swinnen[1,4]

[1]KU Leuven, Movement Control and Neuroplasticity Research Group, Leuven, Belgium
[2]Movement Neuroscience Laboratory, University of Auckland, New Zealand
[3]School of Psychological Sciences and Monash Institute of Cognitive and Clinical Neurosciences, Monash University, Australia
[4]Leuven Research Institute for Neuroscience & Disease (LIND), Leuven, Belgium

---

Abstract: Increasing a participant's ability to prepare for response inhibition is known to result in longer Go response times and is thought to engage a "top-down fronto-striatal inhibitory task set." This premise is supported by the observation of anterior striatum activation in functional magnetic resonance imaging (fMRI) analyses that focus on uncertain versus certain Go trials. It is assumed that setting up a proactive inhibitory task set also influences how participants subsequently implement stopping. To assess this assumption, we aimed to manipulate the degree of proactive inhibition in a modified stop-signal task to see how this manipulation influences activation when reacting to the Stop cue. Specifically, we tested whether there is differential activity of basal ganglia nuclei, namely the subthalamic nucleus (STN) and anterior striatum, on Stop trials when stop-signal probability was relatively low (20%) or high (40%). Successful stopping was associated with increased STN activity when Stop trials were infrequent and increased caudate head activation when Stop trials were more likely, suggesting a different implementation of reactive response inhibition by the basal ganglia for differing degrees of proactive response control. *Hum Brain Mapp 37:4706–4717, 2016.* © 2016 Wiley Periodicals, Inc.

INTRODUCTION

The ability to inhibit responses is fundamental for cognitive control. Sudden changes in the environment can make an action inappropriate or even life threatening. Late movement cancellation mechanisms are thought to rely on *reactive* inhibition, initiated after a stop cue is signaled. However, everyday life often calls for a *proactive* process that anticipates such events on the basis of prior experience [Aron, 2011].

Proactive inhibition can be studied by manipulating stop-signal expectancy from trial-to-trial [Aron et al., 2007; Chikazoe et al., 2009; Zandbelt and Vink, 2010], or at the level of blocks of trials [Federico and Mirabella, 2014; Mirabella et al., 2008; Ramautar et al., 2004; Verbruggen and Logan, 2009b]. These studies have revealed that Go response times increase as a function of stop-signal probability. The magnitude of response slowing has been taken as an index of "proactive inhibition."

Successful *reactive inhibition* is associated with increased activity in a distributed brain network. Two frontal areas, the pre-supplementary motor area (pre-SMA) and the right inferior frontal cortex (rIFC) have been identified as critical for the inhibitory process [for a review see (Aron, 2011)]. However, their precise roles remain equivocal. Whereas some advocate that rIFC has privileged access to the motor system to turn on a brake [Aron et al., 2014], others suggest that preSMA and rIFC are part of domain general networks that control cognitive processes such as attentional control and working memory [Hampshire, 2015; Hampshire and Sharp, 2015], or action planning and execution [Mirabella, 2014], and that successful inhibition emerges from dynamic interactions throughout these networks. fMRI studies have investigated *proactive inhibition* through contrasts of uncertain versus certain Go trials. Their results show that on uncertain Go trials, regions are activated that are typically observed when investigating successful reactive stopping [Chikazoe et al., 2009; Jahfari et al., 2010; Zandbelt et al., 2013; Zandbelt and Vink, 2010], suggesting that the response inhibition network is activated proactively when the likelihood of an upcoming stop is high. Another study used independent component analysis, and identified three common neural networks for proactive and reactive inhibition, but also found evidence for unique neural networks [van Belle et al., 2014].

Besides the cortex, the basal ganglia also play an important role in response inhibition. Competing basal ganglia pathways modulate thalamic-cortical output to inhibit or facilitate cortically initiated movements [Jahanshahi et al., 2015; Schmidt et al., 2013]. As such, the basal ganglia are a strong candidate for the 'agent' of inhibition [Band and van Boxtel, 1999]. For *reactive inhibition*, most studies have focused on the role of the subthalamic nucleus (STN). Functional neuroimaging revealed that stronger STN activation is associated with better inhibitory performance [Aron et al., 2007; Aron and Poldrack, 2006]. STN lesions in rodents resulted in impaired response inhibition [Eagle et al., 2008], and the effects of STN deep brain stimulation in Parkinson's disease strongly suggest that the STN is involved in inhibitory control [Jahanshahi, 2013; Mirabella et al., 2013; Mirabella et al., 2012; Obeso et al., 2013; Swann et al., 2011; van den Wildenberg et al., 2006]. With respect to *proactive inhibition*, comparisons of certain and uncertain Go trials have predominantly revealed increased anterior striatum involvement [Jahfari et al., 2010; Majid et al., 2013; Vink et al., 2005; Zandbelt et al., 2013; Zandbelt and Vink, 2010]. These observations have led to the hypothesis that there might be a differential involvement of STN and the anterior striatum in reactive and proactive inhibition [Aron, 2011].

Yet, even when prior information is provided to indicate the likelihood of stopping and engage the neural mechanisms of proactive inhibition, the stop-signal paradigm and it's dynamic tracking algorithm requires the participant to react quickly to the Stop cue, if and when it appears. Thus the stop process might remain reactive. While important progress has been made toward understanding the neural correlates of proactive inhibition, how this inhibitory task set influences the implementation of response inhibition in the basal ganglia is unknown.

The present experiment was designed to ensure a sufficient number of Stop trials during blocks of high and low stop-signal probability (LSP). This enabled us to test the hypothesis that differential basal ganglia recruitment is evident on successful stop-signal trials when the degree of proactive inhibition was manipulated. Based on the fMRI evidence reviewed above, and the circuits proposed by Aron [2011] [see also Jahanshahi et al. (2015)], we predicted that there would be greater involvement of STN when the probability of stopping was low and greater involvement of the anterior striatum when the probability of stopping was high (Fig. 1).

METHODS

Participants

Participants ($N = 22$, mean age 23.5, 11 male) were right-handed [mean laterality quotient 78.5 (Oldfield, 1971)]. The local ethics committee approved the study, and written informed consent was obtained.

Stop-Signal Paradigm and Experimental Procedure

Participants performed an anticipated response stop-signal task [Coxon et al., 2006; Slater-Hammel, 1960; Zandbelt and Vink, 2010]. The visual display consisted of a vertical indicator that moved from the bottom upwards on each trial (Fig. 2). A target line was situated 800 ms from onset. The primary task was to stop the indicator at the target by releasing the switch (Go trials). Go trials were to be performed as accurately and consistently as possible. To reinforce Go task performance the color of the target line changed to green, yellow, orange or red at the end of the trial, depending on whether responses were within 20, 40, 60, or >60 ms of the target. Sometimes the indicator stopped automatically prior to the target. When this happened, participants tried to prevent releasing the switch (Stop trials). Stop-signal probability was manipulated over blocks: 20% in the LSP condition and 40% in the high stop-signal probability (HSP) condition. Two separate staircasing algorithms ensured convergence to 50% success on Stop trials for LSP and HSP. Initial stop time was determined per individual during the practice session (average 160 ms from target) and was adjusted in steps of 10 ms.

Trials were presented in blocks of ~30s consisting of eight to nine trials. Each block started with a visual
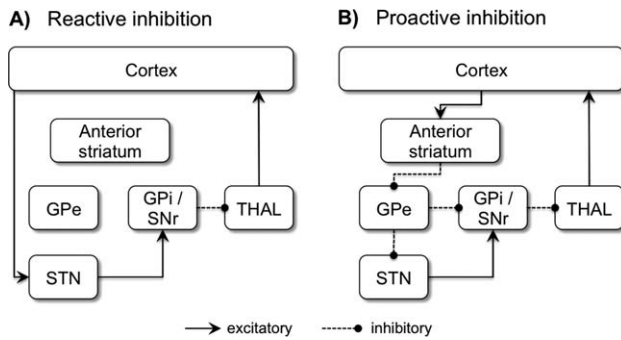
Figure 1.

Hypothetical cortico-basal ganglia pathways mediating reactive and proactive inhibition. (**A**) During reactive inhibition, stop related cortical information (see text for detail on cortical regions involved) might be sent to the STN via the hyperdirect pathway. The STN has an excitatory effect on the GPi/SNr, leading to a suppression of thalamic output to the cortex. (**B**) Proactive inhibitory control might be set up via the indirect pathway. Stop related cortical information is sent to the anterior striatum (caudate and/or putamen), which inhibits activity in the GPe. In turn, the GPe inhibits the GPi (directly or via the STN), resulting in a suppression of thalamic output to the cortex. STN = subthalamic nucleus, GPi = internal segment of the globus pallidus, GPe = external segment of the globus pallidus, SNr = substantia nigra pars reticulata, THAL = thalamus.

instruction cue, visible for 1s, stating whether there was more (HSP) or less (LSP) chance on stopping. Response time was recorded relative to the target on each trial and the indicator was reset to empty after 1s. The inter-trial interval was 3.25s. Indicator color was different for the LSP and HSP blocks (e.g., blue for LSP, magenta for HSP), and this was counterbalanced across participants.

Participants practiced the task by performing one task run outside the scanner to ensure stable performance and determine their initial stop time. Three scanner runs were completed (506 trials in total). The task was presented on a MRI compatible LCD screen and viewed through a double mirror attached to the head coil (input refresh rate 60Hz, image refresh rate 120Hz). To ensure a sufficient number of Stop trials for each condition there were 34 LSP blocks and 25 HSP blocks, resulting in 62 Stop and 244 Go trials for LSP and 80 Stop and 120 Go trials for HSP. An algorithm was used to create pseudorandomized event sequences [Wager and Nichols, 2003].

Behavioral Data Analysis

For each participant, Go trial response times (GoRT) and response times for unsuccessful Stop trials were determined relative to the target (time of response − 800 ms, e.g., if response occurred at 824 ms, then 824–800 = 24 ms after the target). Early response times (>400 ms before the
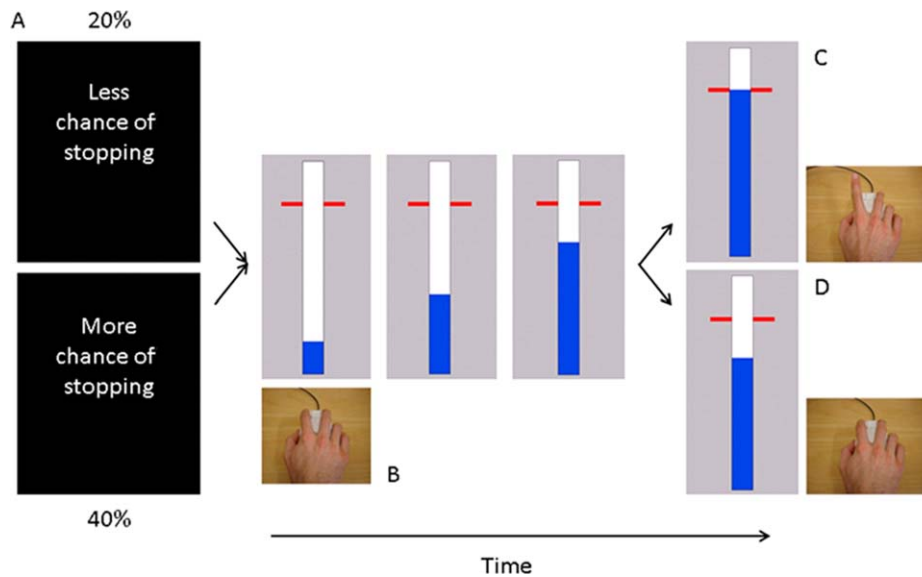

Figure 2.

Behavioral task. (**A**) Each block of trials started with the presentation of an instruction cue (1s) indicating the likelihood of a stop-signal. (**B**) Participants viewed a vertically oriented indicator that increased from the bottom up at constant velocity reaching the top in 1s. The indicator could be stopped by releasing the mouse key with the right index finger. (**C**) Participants were required to stop the indicator as close to the target (800 ms) as possible. (**D**) The bar stopped automatically on 20% (low stop-signal probability condition) or 40% (HSP condition) of the trials. The time at which the bar stopped was adjusted online using two staircase algorithms to achieve 50% success on Stop trials. [Color figure can be viewed at wileyonlinelibrary.com]

target) were considered errors and response times more than 3 SD from mean GoRT were defined as outliers. For Stop trials, the probability of responding was calculated and stop-signal reaction time (SSRT) was determined via the integration method [Verbruggen and Logan, 2009a].

Image Acquisition

A Philips 3T Achieva MRI scanner (Philips Healthcare, The Netherlands) with 32 channel head coil was used for image acquisition. A high resolution T1-weighted structural image was acquired using magnetization prepared rapid gradient echo (MPRAGE; TR = 9.70 ms, TE = 4.60 ms, 230 sagittal slices, $1 \times 0.65 \times 0.65$ mm voxels). A gradient EPI pulse sequence was used for T2*-weighted images (TR = 2s, TE = 30 ms, flip angle = 90°, 34 oblique axial slices, $2.5 \times 2.5 \times 3$ mm voxels, interslice gap 0.2 mm). A fieldmap was acquired using a dual gradient echo acquisition (TR = 750 ms, TE1 = 5.76 ms, TE2 = 7.76 ms, 35 axial slices, $2.5 \times 2.5 \times 4$ mm voxels).

Functional Magnetic Resonance Analysis

fMRI data was analyzed with SPM8 (Wellcome Department of Imaging Neuroscience, University College, London) implemented in MATLAB 7.6 (Mathworks, Sherborn, MA). Images were realigned to the first image, corrected for distortion using the field map, corrected for differences in slice acquisition time by temporal interpolation to the middle slice, coregistered to the anatomical image, and normalized to Montreal Neurological Institute (MNI) space using unified segmentation of the anatomical image. Estimated motion parameters were inspected to ensure translational motion did not exceed 1 voxel. For whole-brain analyses, the normalized functional images were smoothed with a 8mm isotropic FWHM Gaussian kernel. For region of interest analyses, a 4 mm isotropic FWHM Gaussian kernel was used and results were also confirmed without the use of any smoothing to exclude the possibility that partial volume effects were driving the results.fMRI data were analyzed in an event-related design using a General Linear Model with 8 explanatory variables (EVs) of interest, modeled as delta functions at trial onset convolved with the canonical hemodynamic response function and its temporal derivative. Of these, two EVs described Go trials (HSP, LSP). LSP-Go events were randomly sampled to match the number of Go events in the HSP condition (randsample.m function in Matlab). Four EVs described Stop trials (Stop success, SS: HSP, LSP; Stop fail, SF: HSP, LSP), and two EVs described the instruction cues for HSP and LSP. An additional EV modeled events of no interest which included outliers and the remaining LSP Go trials. Realignment parameters, the mean time series from white matter, cerebral spinal fluid, and out of brain voxels were included as covariates of no interest. Data were

filtered in the temporal domain (cutoff of 1/120Hz), and pre-whitened using an AR(1) model.

To test our hypothesis that stop-related activity differed between probability levels in the basal ganglia we specified six anatomical ROI's: left STN, right STN, left anterior putamen, right anterior putamen, left anterior caudate and right anterior caudate. For the STN's we used a probabilistic standard space template based on manual delineation of the STN on susceptibility weighted images [Coxon et al., 2012]. We included both STN's because there is evidence for both right [Aron and Poldrack, 2006] and left [Coxon et al., 2016; Coxon et al., 2012; Ray et al., 2009] STN involvement in reactive inhibition, and bilateral STN deep brain stimulation is often more effective than unilateral stimulation [Mirabella et al., 2012]. The caudate head, and anterior portion of the putamen (defined by axial projection of the anterior commissure [Douaud et al., 2006]) were taken from the Talairach atlas [Lancaster et al., 2000]. These ROIs were chosen based on previous findings of predominantly anterior striatal involvement in proactive inhibition [Majid et al., 2013; Vink et al., 2014; Zandbelt et al., 2013; Zandbelt and Vink, 2010]. Average beta estimates from all voxels within each ROI were extracted by means of Marsbar and subjected to a $6 \times 2 \times$ ANOVA with factors region (left STN, right STN, left anterior putamen, right anterior putamen, left anterior caudate, right anterior caudate), trial type (Go, SS) and stop-signal probability (LSP, HSP). A significant 3-way interaction was followed up by interaction contrasts testing the trial type $\times$ stop-signal probability interaction within each region. Fisher's LSD post hoc tests were used to further describe the pattern of results. A statistical threshold of $P < 0.05$ was applied for all comparisons (Statistica 8, StatSoft, Tulsa, OK). Previous work suggests that the contrast SS > Go might be confounded by perceptual processing of the stop signal [Sharp et al., 2010]. An alternative contrast typically used to isolate inhibition related activity is SS > SF. This contrast assumes however that an inhibitory process is not engaged on failed stop trials, which is highly unlikely. Moreover, this contrast is confounded by differences in attention and reward. By choosing the trial type (SS, Go) $\times$ stop-signal probability interaction (HSP, LSP) as main contrast of interest, we limit the possible confounds because attentional/oddball effects related to the stop signal should be present in both stop-signal probability conditions.

To supplement our hypothesis driven ROI analysis, whole-brain analysis was performed to (1) identify regions with increased activation on Stop trials (Stop > Go), and (2) investigate the effects of stop-signal probability on activation during Go trials at the whole-brain level ($LSP_{Go} > HSP_{Go}$) and ($HSP_{Go} > LSP_{Go}$). Whole-brain statistical inference was corrected for multiple comparisons over the search volume using cluster-level family wise error correction (FWE) at $P < 0.05$ (cluster defining height threshold $t > 3.16$).

TABLE I. Performance characteristics

Trial type		Stop-signal probability			
		LSP (20%)	HSP (40%)	*t*-value	*P*-value
Go	% Errors	0.99 (2.2)	0.53 (1.4)	1.122	0.223
	% Outliers	0.78 (0.6)	0.99 (0.7)	−1.025	0.317
	GoRT (ms)	13.95 (11.9)	19.85 (16.0)	−3.255	0.004
	GoRT Variability (ms)	31.92 (5.9)	36.35 (7.9)	−4.166	<0.001
Stop	Stop fail RT (ms)	−6.07 (10.8)	−1.83 (11.2)	−2.139	0.044
	% Inhibit	48.39 (1.7)	49.37 (1.4)	−3.210	0.004
	SSRT (ms)	188.52 (8.4)	188.21 (9.5)	0.168	0.869

GoRT and Stop fail RT are expressed relative to the target (i.e., response − 800 ms). Early response times (>400 ms before the target) were considered errors and response times more than 3 SD from mean GoRT were defined as outliers. Mean (± standard deviation) and two-tailed paired sample *t*-tests are reported.

RESULTS

Behavioral Results

Table I shows Go and Stop trial performance for both stop-signal probability conditions. The number of errors on Go trials was matched between LSP and HSP [(t(21) = 1.122, P = 0.223]. The dynamic tracking procedure resulted in a stop success rate of 48.4% for LSP and 49.4% for HSP, a subtle yet consistent difference [t(21) = −3.210, P = 0.004]. In line with the literature (see introduction) we observed longer Go response times for HSP than LSP [mean (ms) LSP: 13.95, HSP: 19.85, t(21) = −3.255, P = 0.004] and no difference in SSRT [t(21) = 0.168, P = 0.869], suggesting increased proactive control in the HSP condition. There are however at least two alternative explanations for the difference in response times between the two conditions: (1) automatization toward the go stimulus might have resulted in shorter GoRTs in the LSP condition [Logan, 1988], and (2) accumulation of post stop-signal slowing might result in longer GoRTs in the HSP condition [Bissett and Logan, 2011; Bissett and Logan, 2012].

In the LSP condition there is more opportunity for automatization due to the higher number of Go trial instances and the higher number of Go stimulus presentations (i.e., total number of trials). If automatization toward the go stimulus is driving the results, then GoRT should not differ between the two conditions with the same number of (Go) trials. Comparing the first 120 Go trials from the LSP condition with the 120 Go trials from the HSP condition showed that there was still a significant difference in GoRT [mean (ms) LSP: 16.26, HSP: 20.51, t(21) = −2.186, P = 0.04]. Similarly, GoRT was higher in the HSP condition than the LSP condition when comparing the first 200 trials in the LSP condition to all 200 trials in the HSP condition [mean (ms) LSP: 15.94, HSP: 20.51, t(21) = −2.496, P = 0.021].

To test the hypothesis that an accumulation of post stop-signal slowing could account for the difference in GoRT between the two probability conditions we calculated mean GoRTs for Go trials preceding a Stop trial (S-1) or following a Stop trial (S + 1 and S + 2) for successful (SS) and failed stops (SF) separately (Supporting Information Fig. 1). There was a significant main effect of probability condition [F(1,21) = 20.225, P < 0.001] and time [F(2,42) = 7.836, P = 0.001], and a significant trial type × time interaction [F(2,42) = 18.09, P < 0.001]. For successful stop trials we found no significant difference between response times on SS-1 and SS + 1 trials (post-hoc LSD P = 0.399), but response times were significantly longer in SS + 2 trials than on SS-1 (post-hoc LSD P < 0.001) and SS + 1 trials (post-hoc LSD P < 0.001). Go trial performance after a failed stop (SF + 1, SF + 2) was faster compared to SF-1 performance (post-hoc LSD SF + 1 > SF-1 P = 0.003, SF + 2 > SF-1 P = 0.026). GoRTs on SF + 1 and SF + 2 did not differ (post-hoc LSD 0.427). Importantly, there was no time × stop-signal probability interaction [F(2,42) = 0.244, P = 0.784] and no trial type × time × stop-signal probability interaction [F(2,42) = 0.76, P = 0.472].

fMRI Results

To verify that the previously described 'stopping network' was recruited, we contrasted activity on Stop versus Go trials collapsed across stop-signal probability conditions. As shown previously [Aron and Poldrack, 2006; Coxon et al., 2016], stopping was associated with significant activation in preSMA, anterior cingulate cortex, right IFC pars opercularis (BA44), and bilateral insula. Activation was also evident in left IFC pars orbitalis (BA45), bilateral middle frontal gyrus, supramarginal gyrus, thalamus and caudate extending into a region consistent with the probabilistic standard space template of right STN (shown in green, Fig. 3)(Supporting Information Table I).

The main question addressed in this study was whether there is a distinction between the involvement of STN and the anterior striatum on successful stop-signal trials, i.e., during reactive inhibition, when the level of proactive
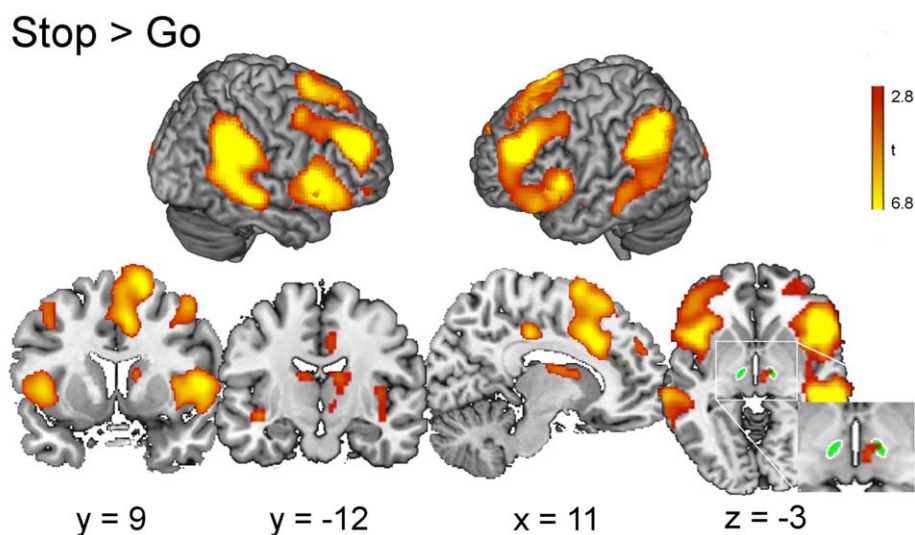
Figure 3.

Brain regions showing more activation during Stop than Go trials. The activation maps include areas previously implicated in response inhibition (right IFC, preSMA, caudate, and STN). The probabilistic standard space template of STN is shown in green. Whole-brain analysis, cluster-level FWE $P < 0.05$, cluster defining height threshold $t > 3.16$. [Color figure can be viewed at wileyonlinelibrary.com]

control was manipulated. The 6x2x2 ANOVA showed a significant 3-way interaction between ROI (left, right STN; left, right anterior putamen; left, right anterior caudate), trial type (Go, SS) and probability condition (LSP, HSP) [$F(5,17) = 7.622$, $P = 0.001$]. Planned contrasts for the trial type $\times$ stop-signal probability condition interaction per ROI revealed significant interactions for left STN [$F(1,21) = 4.922$, $P = 0.038$], and right caudate head [$F(1,21) = 7.953$, $P = 0.010$], but not for right STN, left anterior caudate and left or right anterior putamen ($P > 0.250$). As visualized in Figure 4A left STN was more active during successful stopping for LSP than HSP (LSD post-hoc $LSP_{SS} > HSP_{SS}$: $P < 0.001$), and no difference for $LSP_{Go} > HSP_{Go}$ ($P = 0.188$). In contrast, the right caudate head was more active during successful stopping for HSP than LSP (LSD post-hoc $HSP_{SS} > LSP_{SS}$: $P = 0.016$), but not $HSP_{Go} > LSP_{Go}$ ($P > 0.250$). In a recent paper from de Hollander et al. [2015] concerns are raised about the effect of spatial smoothing (even a minimal smoothing kernel of 4 mm as used here) on the mixture of BOLD signals from the STN and surrounding tissue. Therefore we also tested for the trial type $\times$ probability condition interaction in left and right STN without applying smoothing to the data. There was a similar significant interaction in left STN [$F(1,21) = 4.534$, $P = 0.045$], with higher activity for successful stopping in the LSP condition than HSP (LSD post-hoc $LSP_{SS} > HSP_{SS}$: $P < 0.003$), and no difference for $LSP_{Go} > HSP_{Go}$ ($P = 0.180$). The interaction in right STN was not significant ($P > 0.250$).

In order to compare our manipulation of stop-signal probability with previous studies that investigated proactive inhibition, we also performed whole-brain analysis on Go trials ($HSP_{Go} > LSP_{Go}$). Activation was increased for HSP compared to LSP in bilateral inferior parietal cortex, precuneus and in the right superior and middle frontal gyri (Fig. 4B, Table II). The reverse contrast ($LSP_{Go} > HSP_{Go}$) identified the "default mode network" with more deactivation in the ventral medial prefrontal cortex, posterior cingulate cortex, middle temporal gyrus and inferior parietal cortex for HSP than LSP. This contrast also revealed increased activation for LSP (as opposed to less deactivation) in the insula, hippocampus, temporal pole, and left posterior putamen (Fig. 4B, Table II).

DISCUSSION

We used a mixed block/event-related design to manipulate the degree of proactive inhibition across blocks and investigated how this influenced the implementation of stopping in reaction to a stop cue. The results support a proposed functional distinction between left STN and right anterior striatum on successful stop trials, with a proactive inhibitory task set influencing how reactive inhibition is implemented in the basal ganglia. Moreover, greater uncertainty (HSP) was associated with stronger default mode network (DMN) deactivation and a concurrent increase in fronto-parietal activation, suggesting a role for these large scale networks in proactive inhibition.
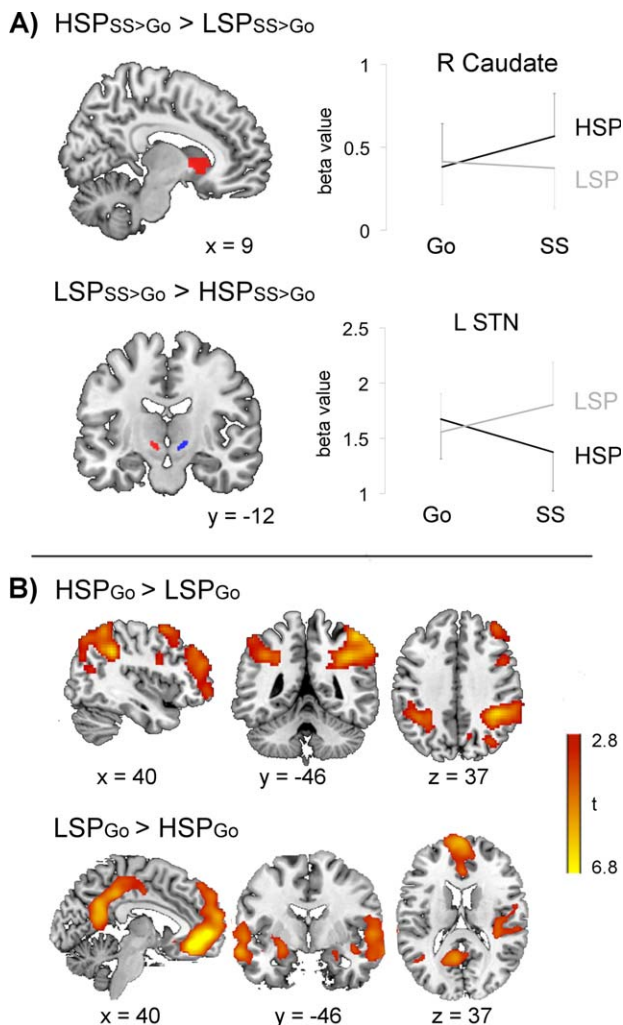
A) HSP_{SS>Go} > LSP_{SS>Go}

x = 9

LSP_{SS>Go} > HSP_{SS>Go}

y = -12

B) HSP_{Go} > LSP_{Go}

x = 40   y = -46   z = 37

LSP_{Go} > HSP_{Go}

x = 40   y = -46   z = 37

Figure 4.

(**A**) Effect of stop-signal probability on stop success activity. ROI analysis. Left: ROIs overlaid on a standard brain. Right: Increased activation was observed in right caudate head during successful stopping for high (HSP) versus the low (LSP) stop-signal probability condition whereas the opposite was observed for the subthalamic nucleus (STN). Plots show the average beta values of all voxels in the ROI (± standard error). (**B**) Effect of stop-signal probability on Go trial activation. Left: Brain regions showing more activation on Go trials for HSP than LSP. Right: Brain regions showing more activation on Go trials for LSP than HSP. Whole-brain analysis, cluster-level FWE $P < 0.05$, cluster defining height threshold $t > 3.16$. [Color figure can be viewed at wileyonlinelibrary.com]

Differential Roles for STN and Anterior Striatum in Response Inhibition

Braver [2012] advocated a framework wherein cognitive control varies along a reactive–proactive continuum. In this framework, the predictability of the environment determines which mechanism is most efficient. In the context of inhibitory control, infrequent presentation of stop-signals creates a strong bias to focus efforts on the Go task [Logan et al., 1984]. A bias toward the Go task can be achieved via a stronger potentiation of the direct basal ganglia pathway to promote (Go) movements [Aron and Poldrack, 2006; Schmidt et al., 2013]. The increased activation of the posterior putamen during Go trials in the low compared to HSP condition could be a reflection of this stronger potentiation (Table II, LSP_{Go} > HSP_{Go}).

On the other hand, frequent presentation of stop-signals shifts priority toward caution. This caution is reflected in longer Go response times in the HSP condition. The behavioral results show that this increase in response time cannot be explained by an instance account, or accumulative post stop-signal slowing, and is therefore likely due to both global and trial-to-trial proactive control adjustments based on stop-signal expectancy. In contrast to previous reports [Bissett and Logan, 2011; Mirabella et al., 2006; Verbruggen et al., 2008] we did not observe post stop-signal slowing on the trial immediately following the stop trial. This might be due to the relatively low occurrence of two stop-signal trials in a row (LSP: 3%, HSP: 22.5%) [Bissett and Logan, 2012] and the implicit and explicit feedback provided on Go task performance in this anticipated response version of the stop-signal task. Interestingly, when two Go trials followed a successful stop trial participants slowed down their response, probably because they anticipated that the likelihood of a stop-signal was high (Supporting Information Fig. 1).

When a stop-signal is presented, a "race" ensues between the triggered Stop process and the already initiated Go process. Inhibition over the Go process could be achieved via the hyperdirect basal ganglia pathway [Nambu et al., 2002], or via the indirect basal ganglia pathway [Mink, 1996]. The hyperdirect pathway consists of excitatory cortical projections toward the STN which causes downstream inhibition of thalamic output toward the cortex. In macaques it has been shown that STN has direct connections with the (pre)motor cortex [Nambu et al., 1997], (pre)SMA [Inase et al., 1999], and the anterior and dorsolateral prefrontal cortex (dlPFC) [Haynes and Haber, 2013]. Diffusion weighted imaging tractography provides complementary evidence in humans and suggests that similar connections exist between rIFC and STN, and pre-SMA and STN [Aravamuthan et al., 2007; Aron et al., 2007; Coxon et al., 2012].

Additional evidence for the existence of a hyperdirect structural pathway comes from studies of STN function during reactive inhibition. Electrophysiological recordings in rats showed that successful reactive stopping requires stop-signal information to be transferred from STN to the basal ganglia output nuclei before the Go process exceeds a point of no return - representing the race between the Stop and the Go process [Schmidt et al., 2013]. In humans, recordings from deep brain stimulation electrodes in STN revealed strong desynchronisation of oscillatory activity in

TABLE II. Stereotactic coordinates of the local maxima

Contrast	Anatomical label	Hemi-sphere	x	y	z	t-value	P-value
$HSP_{Go} > LSP_{Go}$	Inferior parietal cortex/superior parietal cortex/precuneus	R	40	−44	37	6.28	<0.001
			54	−40	55	6.25	
			10	−72	52	6.19	
	Middle frontal gyrus	R	44	48	25	5.26	<0.001
			40	43	40	4.32	
			40	56	−5	3.85	
	Inferior parietal cortex	L	−38	−50	40	4.85	<0.001
			−43	−57	55	4.69	
			−28	−50	37	4.21	
	Superior frontal gyrus	R	37	10	61	4.84	0.001
			24	13	64	4.76	
			42	20	49	3.50	
$LSP_{Go} > HSP_{Go}$	Ventral medial prefrontal cortex / Superior frontal gyrus	L	−3	40	−11	7.71	<0.001
			−18	43	46	5.44	
			−23	26	40	5.34	
	Superior / middle temporal gyrus	L	−63	−4	−14	5.92	<0.001
			−60	−10	−5	5.27	
			−58	−2	−2	5.16	
	Posterior cingulate cortex /precuneus	L	−6	−57	22	5.86	<0.001
			−13	−52	10	5.34	
			−10	−44	40	3.95	
	Insula / hippocampus	L	−26	−34	−5	5.52	0.001
			−28	−20	−17	5.43	
	Posterior putamen		−26	−4	−5	3.83	
	Temporal pole	R	42	−30	22	4.92	<0.001
			62	−4	1	4.91	
			54	0	−2	4.85	
	Inferior parietal cortex	L	−48	−67	25	4.85	0.003

Whole-brain analyses were corrected for multiple comparisons using cluster-level family-wise inference ($P < 0.05$). Stereotactic coordinates are reported in Montreal Neurological Institute (MNI) space. HSP = high stop-signal probability, LSP = low stop-signal probability.

the beta frequency band (15–30 Hz) during movement, which was quickly terminated during successful movement cancelation [Alegre et al., 2013; Ray et al., 2012]. Importantly, this relative increase in beta power took place before SSRT [Bastin et al., 2014]. Cortical recordings have shown a similar increase in beta oscillations in preSMA and rIFC during successful stopping [George et al., 2013; Swann et al., 2011; Swann et al., 2009; Wessel et al., 2013]. Potentially, rIFC increases the influence of preSMA on STN to inhibit thalamo-cortical activity that would have otherwise supported movement execution, as suggested by recent dynamic causal modeling results [Rae et al., 2015]. Consistent with the evidence from electrophysiological recordings, we observed fMRI activation in the STN region on successful Stop trials [Aron and Poldrack, 2006; Coxon et al., 2016].

The stopping network is widely considered as right lateralized [Aron, 2011; Sharp et al., 2010]. However, it remains unclear how a right lateralized network can inhibit movements that are predominantly prepared in the left hemisphere. In the present study, it was left STN that was more active for reactive stopping. Involvement of left STN

in inhibitory control is substantiated by the observation that deep brain stimulation of left STN impairs SSRT in Parkinson's disease patients [Ray et al., 2009]. Moreover, Coxon et al. [2016] showed significant activation in both left and right STN during successful stopping, yet the white matter connections between preSMA and left STN were most strongly related to stopping performance [Coxon et al., 2012]. Based on our results, we tentatively propose that rIFC interacts with left and right STN via preSMA projections in each hemisphere. In the indirect pathway, excitatory projections from the cortex facilitate inhibitory neurons in the striatum. These project to the (external) globus pallidus, which leads to a decrease of tonic inhibition of STN, and therefore to a reduction of thalamic output to the cortex. Evidence for involvement of the indirect pathway in response inhibition comes from the observation that striatal lesions in rats impact inhibitory performance [Eagle and Robbins, 2003]. Moreover, increased striatal activation for successful versus unsuccessful stopping has been associated with shorter SSRTs [Chao et al., 2009] and with the level of M1 activity during successful stopping [Zandbelt and Vink, 2010], suggesting

that striatum could also contribute to the inhibitory function. However, more direct evidence that activity in the striatum is modulated before the SSRT, is lacking.

It has been suggested that the role of the striatum and the indirect pathway might be more proactive. For example, Zandbelt et al. [2013] showed that anterior striatum activation, including the caudate head, is modulated on Go trials as a function of stop-signal probability, and that this relates to the amount of Go response slowing. This observation is consistent with the presumed role for the striatum in proactively setting up the response threshold based on contextual predictions [Bogacz et al., 2010; Forstmann et al., 2010; Lo and Wang, 2006]. Single cell recordings in monkeys have also revealed that caudate is involved in pre-setting basal ganglia circuits during proactive control [Watanabe and Munoz, 2010]. We found increased caudate head activation on successful stop-signal trials for HSP compared to the LSP condition. This might reflect those Stop trials where the response threshold was set particularly high. Increasing the response threshold would lead to longer Go response times, but increased accuracy on Go and Stop trials [Logan et al., 1984]. We observed longer Go response times and a higher stop success rate in the HSP condition, but no significant difference in the percentage of errors on Go trials. A possible explanation could be that Go trial accuracy was already at ceiling level in both conditions (i.e., <1% errors, Table I). Alternatively, the pattern of results can possibly be explained by a delay in the onset of accumulation [Bissett and Logan, 2011; Verbruggen and Logan, 2009b], or by different diffusion models [Dunovan et al., 2015; Logan et al., 2015].

In accordance with previous reports we did not observe differences in SSRT between the proactive (HSP) and reactive (LSP) conditions [Jahfari et al., 2012; Ramautar et al., 2004; Verbruggen and Logan, 2009b; Zandbelt et al., 2013]. Although other studies have reported an improvement in SSRT in the proactive condition [Chikazoe et al., 2009; Smittenaar et al., 2015], this discrepancy could be explained as a trade off. Some participants might slow down on Go trials in order to improve speed, whereas others favor accuracy of inhibition, which may be influenced by the instructions given to the participant [Leotti and Wager, 2010; Smittenaar et al., 2013].

Our finding of (a) increased STN activation on successful stop-signal trials when stop-signals were rare (i.e., LSP > HSP), and (b) increased caudate head activation when stop-signals were relatively frequent (i.e., HSP > LSP), fits with the hypothesis put forward in the literature that the hyperdirect pathway is relatively more involved in reactive inhibition, whereas the indirect pathway is more important for inhibition in a proactive context [Aron, 2011; Jahanshahi et al., 2015]. However, note that the STN is also part of the indirect pathway. Therefore, no strong conclusions can be made with respect to the pathway taken. Indeed, human electrophysiological recordings

have shown that STN local field potential power was also increased on Go trials for which stopping was anticipated, although to a lesser degree than during reactive stopping [Benis et al., 2014]. Further, STN stimulation can result in an improvement of proactive control in Parkinson's disease patients [Mirabella et al., 2013; Obeso et al., 2013]. In our study, STN effect sizes (Fig. 2B, compare STN beta values on Go trials) were also slightly higher for Go trials in the HSP condition than in LSP, although not significantly. The difference in activity level might be too small to pick up with fMRI.

Proactive Control as a Brain State

When contrasting Go trials for HSP versus LSP we did not observe increased activation of the anterior striatum, preSMA, and rIFC as previously reported [Chikazoe et al., 2009; Jahfari et al., 2010; Zandbelt et al., 2013; Zandbelt and Vink, 2010], but we do not consider this to undermine the results of our experiment. Notably, these studies either contrasted 0% versus 20% stop-signal probability, or looked for a linear increase in activation with stop-signal probabilities ranging from 0–33%. Comparison with a "certain" Go (0% stop-signals) condition may be necessary to observe activation in rIFC and preSMA associated with proactive inhibition on Go trials. We did not include a 0% stop-signal probability condition in our design, instead contrasting relatively low (LSP 20%) and high (HSP 40%) stop-signal conditions. Proactive control mechanisms might still have been recruited to some extent for our LSP condition with fMRI not being sensitive enough to pick up the difference with HSP, in accordance with Ramautar et al. [2006] and Jahfari et al. [2012].

We did observe increased activation in the fronto-parietal network on Go trials for HSP versus LSP. Specifically, activation of right dlPFC, superior/inferior parietal cortex, and precuneus was associated with our manipulation of proactive inhibition. A parietal network uniquely associated with proactive inhibition was previously identified by van Belle et al. [2014]. The dlPFC is connected to the caudate head [Alexander et al., 1986] and has been implicated in proactive inhibitory control. Aron [2011] suggested that dlPFC might be involved in holding more information in working memory during proactive inhibitory control, although in our design two task goals needed to be maintained for both probability conditions. The dlPFC has also been suggested to play a role in goal-directed behavior, presetting fronto-basal ganglia pathways based on current action goals [Bogacz et al., 2010; Miller, 2000; van Veen et al., 2008].

The reverse contrast, $LSP_{Go} > HSP_{Go}$ included parts of the DMN, and this was due to stronger deactivation of the posterior cingulate cortex and ventral medial prefrontal cortex in the HSP condition. Stronger deactivation of the DMN is observed with increased cognitive demands [Singh and Fawcett, 2008], suggesting that behavior in the

HSP condition is less automatic and requires more top down control. Failure to appropriately deactivate the DMN is associated with impairments in inhibitory control [Bonnelle et al., 2012]. Leech et al. [2012] have suggested that stronger deactivation of the DMN might allow more stable, sustained processing in other networks such as the fronto-parietal network. Other regions showed increased activation for this contrast with the insula, inferior frontal and temporal regions were more active during Go trials in LSP. These regions are considered the core nodes in the ventral attention or salience network. They might help to activate the fronto-parietal network in response to unexpected events [Corbetta et al., 2008]. Based on these observations we propose that proactive inhibitory control can also be seen as a 'brain state', involving more sustained attentional focus, while keeping track of the contextual probabilities to preset basal ganglia circuits.

In conclusion, our design made it possible to test the effect of inhibitory task set on basal ganglia recruitment during reactive inhibitory control. The data supports the hypothesis that STN is essential for reactive inhibition, but that caudate head may play a greater role when reactive inhibition occurs in the presence of enhanced proactive control.

ACKNOWLEDGMENTS

REFERENCES

Alegre M, Lopez-Azcarate J, Obeso I, Wilkinson L, Rodriguez-Oroz MC, Valencia M, Garcia-Garcia D, Guridi J, Artieda J, Jahanshahi M, Obeso JA (2013): The subthalamic nucleus is involved in successful inhibition in the stop-signal task: A local field potential study in Parkinson's disease. Exp Neurol 239: 1–12.

Alexander GE, DeLong MR, Strick PL (1986): Parallel organization of functionally segregated circuits linking basal ganglia and cortex. Ann Rev Neurosci 9:357–381.

Aravamuthan BR, Muthusamy KA, Stein JF, Aziz TZ, Johansen-Berg H (2007): Topography of cortical and subcortical connections of the human pedunculopontine and subthalamic nuclei. Neuroimage 37:694–705.

Aron AR (2011): From reactive to proactive and selective control: Developing a Richer model for stopping inappropriate responses. Biol Psychiatry 69:E55–E68.

Aron AR, Behrens TE, Smith S, Frank MJ, Poldrack RA (2007): Triangulating a cognitive control network using diffusion-weighted magnetic resonance imaging (MRI) and functional MRI. J Neurosci 27:3743–3752.

Aron AR, Poldrack RA (2006): Cortical and subcortical contributions to stop signal response inhibition: Role of the subthalamic nucleus. J Neurosci 26:2424–2433.

Aron AR, Robbins TW, Poldrack RA (2014): Inhibition and the right inferior frontal cortex: One decade on. Trend Cogn Sci 18:177–185.

Band GPH, van Boxtel GJM (1999): Inhibitory motor control in stop paradigms: Review and reinterpretation of neural mechanisms. Acta Psychol 101:179–211.

Bastin J, Polosan M, Benis D, Goetz L, Bhattacharjee M, Piallat B, Krainik A, Bougerol T, Chabardes S, David O (2014): Inhibitory control and error monitoring by human subthalamic neurons. Transl Psychiatry 4:e439.

Benis D, David O, Lachaux JP, Seigneuret E, Krack P, Fraix V, Chabardes S, Bastin J (2014): Subthalamic nucleus activity dissociates proactive and reactive inhibition in patients with Parkinson's disease. Neuroimage 91:273–281.

Bissett PG, Logan GD (2011): Balancing cognitive demands: Control adjustments in the stop-signal paradigm. J Exp Psychol Learn Mem Cogn 37:392–404.

Bissett PG, Logan GD (2012): Post-stop-signal slowing: Strategies dominate reflexes and implicit learning. J Exp Psychol Hum Percept Perform 38:746–757.

Bogacz R, Wagenmakers EJ, Forstmann BU, Nieuwenhuis S (2010): The neural basis of the speed-accuracy tradeoff. Trend Neurosci 33:10–16.

Bonnelle V, Ham TE, Leech R, Kinnunen KM, Mehta MA, Greenwood RJ, Sharp DJ (2012): Salience network integrity predicts default mode network function after traumatic brain injury. Proc Natl Acad Sci U S A 109:4690–4695.

Braver TS (2012): The variable nature of cognitive control: A dual mechanisms framework. Trend Cogn Sci 16:106–113.

Chao HHA, Luo X, Chang JLK, Li CSR (2009): Activation of the pre-supplementary motor area but not inferior prefrontal cortex in association with short stop signal reaction time—An intra-subject analysis. Bmc Neuroscience 10:

Chikazoe J, Jimura K, Hirose S, Yamashita K, Miyashita Y, Konishi S (2009): Preparation to inhibit a response complements response inhibition during performance of a stop-signal task. J Neurosci 29:15870–15877.

Corbetta M, Patel G, Shulman GL (2008): The reorienting system of the human brain: From environment to theory of mind. Neuron 58:306–324.

Coxon JP, Goble DJ, Leunissen I, Van Impe A, Wenderoth N, Swinnen SP (2016): Functional brain activation associated with inhibitory control deficits in older adults. Cereb Cortex 26: 12–22.

Coxon JP, Stinear CM, Byblow WD (2006): Intracortical inhibition during volitional inhibition of prepared action. J Neurophysiol 95:3371–3383.

Coxon JP, Van Impe A, Wenderoth N, Swinnen SP (2012): Aging and inhibitory control of action: Cortico-subthalamic connection strength predicts stopping performance. J Neurosci 32:8401–8412.

de Hollander G, Keuken MC, Forstmann BU (2015): The subcortical cocktail problem; mixed signals from the subthalamic nucleus and substantia nigra. PLoS One 10:e0120572.

Douaud G, Gaura V, Ribeiro MJ, Lethimonnier F, Maroy R, Verny C, Krystkowiak P, Damier P, Bachoud-Levi AC, Hantraye P, Remy P (2006): Distribution of grey matter atrophy in Huntington's disease patients: A combined ROI-based and voxel-based morphometric study. Neuroimage 32:1562–1575.

Dunovan K, Lynch B, Molesworth T, Verstynen T (2015): Competing basal ganglia pathways determine the difference between stopping and deciding not to go. Elife 4:e08723.

Eagle DM, Baunez C, Hutcheson DM, Lehmann O, Shah AP, Robbins TW (2008): Stop-signal reaction-time task performance: Role of prefrontal cortex and subthalamic nucleus. Cerebral Cortex 18:178–188.

Eagle DM, Robbins TW (2003): Inhibitory control in rats performing a stop-signal reaction-time task: Effects of lesions of the medial striatum and d-amphetamine. Behav Neurosci 117:1302–1317.

Federico P, Mirabella G (2014): Effects of probability bias in response readiness and response inhibition on reaching movements. Exp Brain Res 232:1293–1307.

Forstmann BU, Anwander A, Schafer A, Neumann J, Brown S, Wagenmakers EJ, Bogacz R, Turner R (2010): Cortico-striatal connections predict control over speed and accuracy in perceptual decision making. Proc Natl Acad Sci U S A 107: 15916–15920.

George JS, Strunk J, Mak-McCully R, Houser M, Poizner H, Aron AR (2013): Dopaminergic therapy in Parkinson's disease decreases cortical beta band coherence in the resting state and increases cortical beta band power during executive control. Neuroimage Clin 3:261–270.

Hampshire A (2015): Putting the brakes on inhibitory models of frontal lobe function. Neuroimage 113:340–355.

Hampshire A, Sharp DJ (2015): Contrasting network and modular perspectives on inhibitory control. Trends Cogn Sci 19: 445–452.

Haynes WIA, Haber SN (2013): The organization of prefrontal-subthalamic inputs in primates provides an anatomical substrate for both functional specificity and integration: Implications for basal ganglia models and deep brain stimulation. J Neurosci 33:4804–4814.

Inase M, Tokuno H, Nambu A, Akazawa T, Takada M (1999): Corticostriatal and corticosubthalamic input zones from the presupplementary motor area in the macaque monkey: Comparison with the input zones from the supplementary motor area. Brain Res 833:191–201.

Jahanshahi M (2013): Effects of deep brain stimulation of the subthalamic nucleus on inhibitory and executive control over prepotent responses in Parkinson's disease. Front Syst Neurosci 7:118.

Jahanshahi M, Obeso I, Rothwell JC, Obeso JA (2015): A fronto-striato-subthalamic-pallidal network for goal-directed and habitual inhibition. Nat Rev Neurosci 16:719–732.

Jahfari S, Stinear CM, Claffey M, Verbruggen F, Aron AR (2010): Responding with restraint: What are the neurocognitive mechanisms? J Cogn Neurosci 22:1479–1492.

Jahfari S, Verbruggen F, Frank MJ, Waldorp LJ, Colzato L, Ridderinkhof KR, Forstmann BU (2012): How preparation changes the need for top-down control of the basal ganglia when inhibiting premature actions. J Neurosci 32: 10870–10878.

Lancaster JL, Woldorff MG, Parsons LM, Liotti M, Freitas CS, Rainey L, Kochunov PV, Nickerson D, Mikiten SA, Fox PT (2000): Automated Talairach atlas labels for functional brain mapping. Hum Brain Mapp 10:120–131.

Leech R, Braga R, Sharp DJ (2012): Echoes of the brain within the posterior cingulate cortex. J Neurosci 32:215–222.

Leotti LA, Wager TD (2010): Motivational influences on response inhibition measures. J Exp Psychol Hum Percept Perform 36: 430–447.

Lo CC, Wang XJ (2006): Cortico-basal ganglia circuit mechanism for a decision threshold in reaction time tasks. Nat Neurosci 9: 956–963.

Logan GD (1988): Toward an instance theory of automatization. Psychol Rev 95:492–527.

Logan GD, Cowan WB, Davis KA (1984): On the ability to inhibit simple and choice reaction time responses: A model and a method. J Exp Psychol-Hum Percept Perform 10:276–291.

Logan GD, Yamaguchi M, Schall JD, Palmeri TJ (2015): Inhibitory control in mind and brain 2.0: Blocked-input models of saccadic countermanding. Psychol Rev 122:115–147.

Majid DSA, Cai WD, Corey-Bloom J, Aron AR (2013): Proactive selective response suppression is implemented via the basal ganglia. J Neurosci 33:13259–13269.

Miller EK (2000): The prefrontal cortex and cognitive control. Nat Rev Neurosci 1:59–65.

Mink JW (1996): The basal ganglia: Focused selection and inhibition of competing motor programs. Prog Neurobiol 50:381–425.

Mirabella G (2014): Should I stay or should I go? Conceptual underpinnings of goal-directed actions. Front Syst Neurosci 8:206.

Mirabella G, Iaconelli S, Modugno N, Giannini G, Lena F, Cantore G (2013): Stimulation of subthalamic nuclei restores a near normal planning strategy in Parkinson's patients. PLoS One 8: e62793.

Mirabella G, Iaconelli S, Romanelli P, Modugno N, Lena F, Manfredi M, Cantore G (2012): Deep brain stimulation of subthalamic nuclei affects arm response inhibition in Parkinson's patients. Cerebral Cortex 22:1124–1132.

Mirabella G, Pani P, Ferraina S (2008): Context influences on the preparation and execution of reaching movements. Cogn Neuropsychol 25:996–1010.

Mirabella G, Pani P, Pare M, Ferraina S (2006): Inhibitory control of reaching movements in humans. Exp Brain Res 174:240–255.

Nambu A, Tokuno H, Inase M, Takada M (1997): Corticosubthalamic input zones from forelimb representations of the dorsal and ventral divisions of the premotor cortex in the macaque monkey: Comparison with the input zones from the primary motor cortex and the supplementary motor area. Neurosci Lett 239:13–16.

Nambu A, Tokuno H, Takada M (2002): Functional significance of the cortico-subthalamo-pallidal 'hyperdirect' pathway. Neurosci Res 43:111–117.

Obeso I, Wilkinson L, Rodriguez-Oroz MC, Obeso JA, Jahanshahi M (2013): Bilateral stimulation of the subthalamic nucleus has differential effects on reactive and proactive inhibition and conflict-induced slowing in Parkinson's disease. Exp Brain Res 226:451–462.

Oldfield RC (1971): Assessment and analysis of handedness—Edinburgh inventory. Neuropsychologia 9:97–113.

Rae CL, Hughes LE, Anderson MC, Rowe JB (2015): The prefrontal cortex achieves inhibitory control by facilitating subcortical motor pathway connectivity. J Neurosci 35:786–794.

Ramautar JR, Kok A, Ridderinkhof KR (2004): Effects of stop-signal probability in the stop-signal paradigm: The N2/P3 complex further validated. Brain Cogn 56:234–252.

Ramautar JR, Slagter HA, Kok A, Ridderinkhof KR (2006): Probability effects in the stop-signal paradigm: The insula and the significance of failed inhibition. Brain Res 1105:143–154.

Ray NJ, Brittain JS, Holland P, Joundi RA, Stein JF, Aziz TZ, Jenkinson N (2012): The role of the subthalamic nucleus in response inhibition: Evidence from local field potential recordings in the human subthalamic nucleus. Neuroimage 60: 271–278.

Ray NJ, Jenkinson N, Brittain J, Holland P, Joint C, Nandi D, Bain PG, Yousif N, Green A, Stein JS, Aziz TZ (2009): The role of the subthalamic nucleus in response inhibition: Evidence from deep brain stimulation for Parkinson's disease. Neuropsychologia 47:2828–2834.

Schmidt R, Leventhal DK, Mallet N, Chen FJ, Berke JD (2013): Canceling actions involves a race between basal ganglia pathways. Nat Neurosci 16:1118–U194.

Sharp DJ, Bonnelle V, De Boissezon X, Beckmann CF, James SG, Patel MC, Mehta MA (2010): Distinct frontal systems for response inhibition, attentional capture, and error processing. Proc Natl Acad Sci U S A 107:6106–6111.

Singh KD, Fawcett IP (2008): Transient and linearly graded deactivation of the human default-mode network by a visual detection task. Neuroimage 41:100–112.

Slater-Hammel AT (1960): Reliability, accuracy, and refractoriness of a transit reaction. Res Quarter 31:217–228.

Smittenaar P, Guitart-Masip M, Lutti A, Dolan RJ (2013): Preparing for selective inhibition within frontostriatal loops. J Neurosci 33:18087–18097.

Smittenaar P, Rutledge RB, Zeidman P, Adams RA, Brown H, Lewis G, Dolan RJ (2015): Proactive and reactive response inhibition across the lifespan. PLoS One 10:e0140383.

Swann N, Poizner H, Houser M, Gould S, Greenhouse I, Cai WD, Strunk J, George J, Aron AR (2011): Deep brain stimulation of the subthalamic nucleus alters the cortical profile of response inhibition in the beta frequency band: A scalp EEG study in Parkinson's disease. J Neurosci 31:5721–5729.

Swann N, Tandon N, Canolty R, Ellmore TM, McEvoy LK, Dreyer S, DiSano M, Aron AR (2009): Intracranial EEG reveals a time- and frequency-specific role for the right inferior frontal gyrus and primary motor cortex in stopping initiated responses. J Neurosci 29:12675–12685.

van Belle J, Vink M, Durston S, Zandbelt BB (2014): Common and unique neural networks for proactive and reactive response inhibition revealed by independent component analysis of functional MRI data. Neuroimage 103:65–74.

van den Wildenberg WPM, van Boxtel GJM, van der Molen MW, Bosch DA, Speelman JD, Brunia CHM (2006): Stimulation of the subthalamic region facilitates the selection and inhibition of motor responses in Parkinson's disease. J Cogn Neurosci 18: 626–636.

van Veen V, Krug MK, Carter CS (2008): The neural and computational basis of controlled speed-accuracy tradeoff during task performance. J Cogn Neurosci 20:1952–1965.

Verbruggen F, Logan GD (2009a): Models of response inhibition in the stop-signal and stop-change paradigms. Neurosci Biobehav Rev 33:647–661.

Verbruggen F, Logan GD (2009b): Proactive adjustments of response strategies in the stop-signal paradigm. J Exp Psychol Hum Percept Perform 35:835–854.

Verbruggen F, Logan GD, Liefooghe B, Vandierendonck A (2008): Short-term aftereffects of response inhibition: Repetition priming or between-trial control adjustments? J Exp Psychol Hum Percept Perform 34:413–426.

Vink M, Kahn RS, Raemaekers M, van den Heuvel M, Boersma M, Ramsey NF (2005): Function of striatum beyond inhibition and execution of motor responses. Hum Brain Mapp 25:336–344.

Vink M, Zandbelt BB, Gladwin T, Hillegers M, Hoogendam JM, van den Wildenberg WP, Du Plessis S, Kahn RS (2014): Frontostriatal activity and connectivity increase during proactive inhibition across adolescence and early adulthood. Hum Brain Mapp 35:4415–4427.

Wager TD, Nichols TE (2003): Optimization of experimental design in fMRI: A general framework using a genetic algorithm. Neuroimage 18:293–309.

Watanabe M, Munoz DP (2010): Presetting basal ganglia for volitional actions. J Neurosci 30:10144–10157.

Wessel JR, Conner CR, Aron AR, Tandon N (2013): Chronometric electrical stimulation of right inferior frontal cortex increases motor braking. J Neurosci 33:19611–19619.

Zandbelt BB, Bloemendaal M, Neggers SFW, Kahn RS, Vink M (2013): Expectations and violations: Delineating the neural network of proactive inhibitory control. Hum Brain Mapp 34:2015–2024.

Zandbelt BB, Vink M (2010): On the role of the striatum in response inhibition. Plos One 5: